RAM ROBOTICS AND MECHATRONICS

DESIGN OF A 3D PRINTED ACTUATION PLATFORM FOR CONCENTRIC TUBE ROBOTS

G. (Georgios) Gkovopoulos

MSC ASSIGNMENT

Committee:
prof. dr. ir. S. Stramigioli
ir. A.G. de Groot
dr. F.J. Siepel
ir. E.E.G. Hekman

June, 2022

019RaM2022
Robotics and Mechatronics
EEMCS
University of Twente
P.O. Box 217
7500 AE Enschede
The Netherlands

UNIVERSITY OF TWENTE. | TECHMED CENTRE UNIVERSITY OF TWENTE. | DIGITAL SOCIETY INSTITUTE

Design of 3D Printed Actuation Unit for Concentric Tube Robots

Georgios Gkovopoulos

June 16, 2022

Contents

1 Introduction

Bladder cancer currently stands in the top ten most common types of cancer around the globe while, the risk of developing urinary bladder cancer in their lifetime is 1,1% for men and 0.27% for women [14]. Cystoscopy is one of the most common procedures to evaluate lower urinary tract diseases [19] and plays an important role in both diagnosis and treatment as well as the follow-up of patients. Currently cystoscopy makes use of 2D images [9] from which the attending physician keeps notes and the results of each cystoscopy are documented in written form, which in many cases can lead to problems in communication between medical personnel and less quantitative results in general[13]. Towards the inspection of the bladder and the detection and localization of any tumours/lesions, a promising approach is the internal inspection using cameras and providing live feed and/or 3D reconstruction of the bladder surface to the doctors or surgeons. Thus digital mapping of the bladder promises great results in appropriately handling the disease [13], [9].

The camera is inserted in the body through the urinary tract using miniature continuum type robots through their use as flexible endoscopes [9]. The use of continuum type robots is currently evolving regarding their application in medical settings [4], [22]. They differ from their linear counterparts as they tend to have more degrees of freedom which allows them to move through confined spaces more easily and their actuation generally does not affect their size making them a great tool for minimally invasive surgery (MIS) [22]. In addition the use of flexible robots instead of rigid ones greatly reduces the patient discomfort during the procedure due to their small size relative to the conventionally used catheters. [19]. These robots are classified based on their motion system in different categories such as continuously-bending, tendon-driven, concentric tube, steerable needle robots etc.

The present project focuses on concentric tube robots namely for their use in bladder cancer detection. They possess advantages over tendon-driven robots, which have also been used in endoscopic processes, as their actuation units tend to be less bulky [22] and their bodies are also slimmer than other continuum robot designs [4] allowing them to enter the body through smaller holes and affect less the surrounding live tissue. These robots consist of a sequence of telescopic precurved tubes made from super elastic nickel-titanium alloy (super elastic nitinol), where one tube is inserted into the next. Figure 1a demonstrates a CAD design of the frontal end of the tubes. Figure 1b shows the size difference of a CTR and the commercially used DaVinci robot end-effector and illustrates further the reason CTRs are considered prime candidates for MIS. The hollow shaft of the tubes can accommodate cables for controlling articulated tools for surgery or even small cameras for inspection purposes.

The two main areas of research for these robots are the design of the actuation unit and the kinematic modelling of the tubes which is used to control the pose of the end-effector of the robot as well as its overall shape. The kinematic modelling of these robots can be quite challenging since the final model needs to be both precise (in order to be able to accurately predict pose changes)

(a) CAD Design of Concentric Tubes [1]

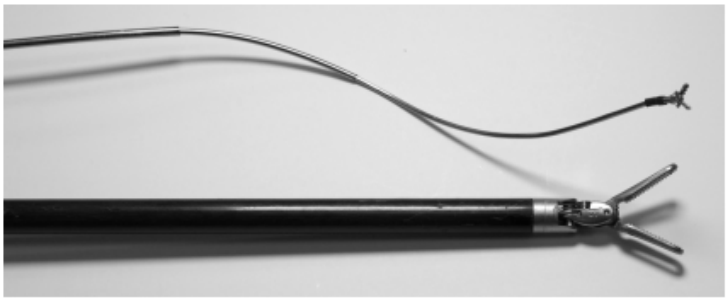

(b) Size comparison between a CTR and DaVinci robot end-effector [11]

but also computationally cheap in order to be suitable for real time operation. A variety of mechanical phenomena affect the modelling such as torsion, bending, non-linear elasticity and friction and are the main reasons for modelling inaccuracies. The kinematic modelling of CTRs has seen a bigger development relative to the development of the actuation unit [1] and in most cases the prototype design is not motivated enough and results in a precise yet complex and expensive realization.

An overview of the different prototype realizations from literature provides a broader understanding of the available solutions for different topics regarding the actuation unit design. Such prototypes have been designed for a multitude of different medical operations such as skull base surgery [5], single nostril skull base surgery [17], transoral lung access system [18], transurethral laser prostate surgery [12] and vitrectomy [10] among others. The actuation of these tubes takes place in their proximal end where translation and rotation of the tubes occurs. By controlling translation and rotation of the tubes the overall shape of the robot can be controlled along with the end-effector pose. The actuation of CTRs has been achieved in different ways ranging from electromechanical ([5],[17],[18],[21], [12], [10]), to pneumatic ([6], [7]) , to piezoelectric actuation ([15],[16]). The previously illustrated prototypes have been created for a multitude of medical operations, using different actuation methods and with a wide range of DoFs. They also differ in their control strategies, as some use closed feedback control with the use of encoder, magnetic or MRI data and finally they could be MRI-compatible or not depending on the materials used. It is quite obvious that the design of these prototypes can follow many paths

that depend on the target application as well as the designers' own choices.

The current work proposes the conceptual design and prototyping of a modular actuation unit platform for a concentric tube robot focused on a motivated approach. More specifically we will focus on how we can create a CTR for use in bladder cancer detection that achieves submillimeter precision while also being cost-effective to manufacture? What are the parameters of the design that affect the accuracy and precision of the final robot design? How can we optimize the design for compactness and relative ease of use? In chapter 2 general design considerations that constitute the common ground of designing an actuation unit for a CTR will be discussed. A literature overview of these subjects will lead to initial decisions about the prototype considering the effect they have on the aforementioned aims of this project. In chapter 3 the realization of the prototype will be presented along with the practical solutions employed. In chapter 4 the experimental procedures will be presented along with their results in determining the accuracy and the precision of the prototype. Finally, in chapter 5, a discussion will ensue about the obtained experiment results as well as the general approaches utilised for developing the prototype. Finally in chapter 6, conclusions for the developed prototype will be derived along with directive lines for possible future work.

2 Design Considerations

In this chapter the general decisions of the upcoming prototype design will be derived and motivated. These choices include actuation chain and general motor choice, translation and rotation realization, sensing and cannula fastening. The aim is to demonstrate the solutions employed in the literature while also motivating the choices made for the current prototype based on the general target requirements. The initial design targets involve accuracy and precision requirements, compactness, general design simplicity and cost effectiveness. Initial literature review of the aforementioned aspects will lead to design decisions made for the presented prototype.

2.1 Actuation Chain

The actuation chain (also referred to as kinematic chain) can take two forms according to literature, serial and parallel [3]. Figure 2 illustrates the two different ways of actuation. In a serial actuation chain all the translating blocks share the same axis of translation while in a parallel actuation chain each translating block operates on each own axis. The most commonly used design is the serial one because the parallel design tends to be more complicated [3]. In addition to having increased complexity, parallel actuation results in both bulkier and heavier designs in general due to increased number of components required for its realization, e.g. any guiding element that allows translational movement in one direction in cartesian space (while disallowing movement in other directions) is required threefold in a parallel actuation realization. One advantage of employ-

ing parallel actuation is that it allows for shorter tubes due to smaller distance between sequential actuation blocks. Such an effect is illustrated in figure 2 as the proximal end of the tubes are closer to each other than the serial case. from a practical standpoint, shorter tubes means lower cost while also allowing for less total energy to be stored in the tubes due to deformation resulting from two tubes rotating in relation to each other.

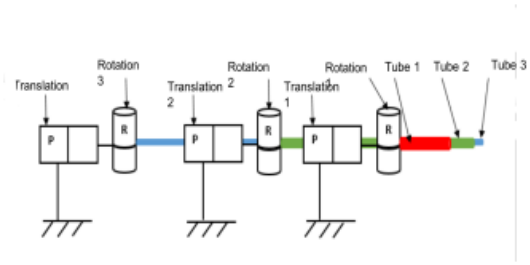

(a) Serial Actuation Chain

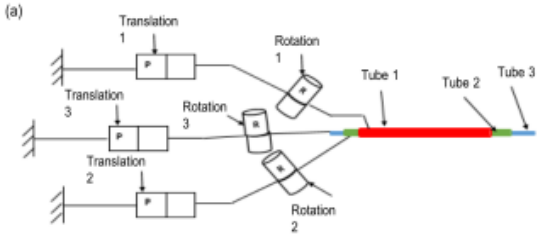

(b) Parallel Actuation Chain

Figure 2: Actuation chain realizations in CTRs [1]

2.2 Actuation & General Motor Choice

In literature both piezoelectric and pneumatic actuation have been used with relative success regarding the accuracy/precision results reported. The use of such actuation types renders the design MRI-compatible which in turn allows for feedback control of the robot's end effector, however the complexity and cost of the design increases as control strategies are more complicated and general components (referring to motors, drivers etc.) tend to be more more expensive.

Electromechanical is the most widely used type of actuation for these prototypes. It is relatively simpler to achieve and utilizes components that are more cost effective than the other two actuation types while their precision is adequate when considering the application. It is worth noting however that a design employing electromechanical actuation is not MRI-compatible due to the introduction of ferromagnetic materials. The two dominant choices of motors

in the literature for these prototypes are DC brushless motors and stepper motors. DC brushless motors are generally durable, precise and efficient however they are relatively more difficult to control than steppers due to the need of encoders to establish feedback control. Stepper motors provide relatively accurate positioning and speed control (they are also used in applications like CNC and 3D printing where high positional accuracy is required) while they do not require feedback control to achieve necessary precision. They have good characteristics at low speeds and high holding torque, however their torque decays at high speeds, they will generate more noise during operation compared to DC brushless motors and require constant maximum current consumption during their operation in order to sustain their specified holding torque. At high loads/speeds the stepper motors might also skip steps. Generally both of the motor have low cost and are quite reliable while also being relatively precise under correct control schemes. In essence both motor choices are viable for the target requirements of the proposed prototype. In the continuation of this chapter piezoelectric and pneumatic actuation choices will not be illustrated since their implementation steers the prototype away from the target requirements of both complexity and cost effectiveness.

2.3 Translation & Rotation

Translation of CTR modules using electric motors has been achieved in different ways in literature. Motorized linear slides have been employed by [21],[20]. Although a compact and efficient solution from a practical point of view, this solution tends to be quite expensive considering alternatives. These motorized slides achieve translation using stepper or BLDC motors and include a sliding element along with control and sensoring equipment. Alternatives included non captive stepper motors on lead screws and a linear rail [10] and non captive stepper motors on a lead thread on a panel sliding on guide rods ([8]).

To achieve rotation of the tubes the use of motorized rotary stages is again an option, but again although compact and precise are not cost-effective solutions. Electric motors with the use of a pulley system [8] or the use of gears [2] is a prominent choice for rotation in literature. In [10] the design employs the use of hollow stepper motors where the cannulas pass through the rotor and their rotational motion is coupled with the rotor's motion which constitutes a solution with the less components.

2.4 Sensing

The need for sensing is heavily affected from the choice of motors. In the case of DC brushless as well as general pneumatic and piezoelectric actuation the need for sensing is prominent since encoders are required for closed loop control. In the case of stepper motors however encoder sensing is not necessary however it has been employed by [10] and [8]. Furthermore, force sensors and/or photointerruptors could be used for alignment and homing operations respectively. In [2] the prototype utilizes photointerruptors to implement translational and

rotational homing sequences for the robot. This interesting approach aims at ensuring that the stages always begin their operation from the same point. This addition increases the repeatability capability of the device and sets a basis for the accuracy of the unit. In [21] the authors use a 6-DoF force/torque sensor (located at the base of the inner tube) to align the tubes in a way where the force(/torque) feedback is minimum. This guarantees that the system has knowledge of the current tube orientation and has the ability through specified software to align the tubes if needed on startup adding to the robot's rotational accuracy.

2.5 Cannula Fastening

The solutions for cannula fastening have been quite diverse in the literature. Fastening the cannulas has been accomplished in the literature with the use of collets [5]. In this case, different collet diameters would be required to fasten tubes with different diameters but generally collets are quite inexpensive and versatile. In figure 4 the employed solution can be seen. In other cases, the tubes were bonded on their back end in either cylindrical brass housings [17] or simple nuts that are then attached to each stage and to the system that provides the rotation of the tubes. Figure 3 shows how the housing of the tubes was implemented by [17].

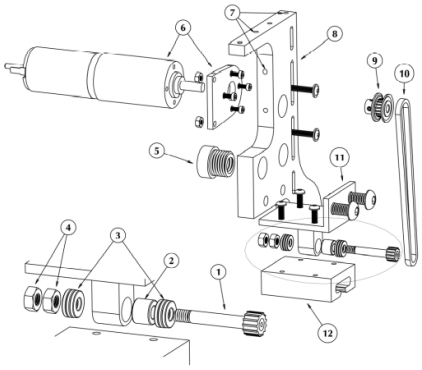

Figure 3: Cannula fastening solution using brass housing (pointers 1-4) [17]

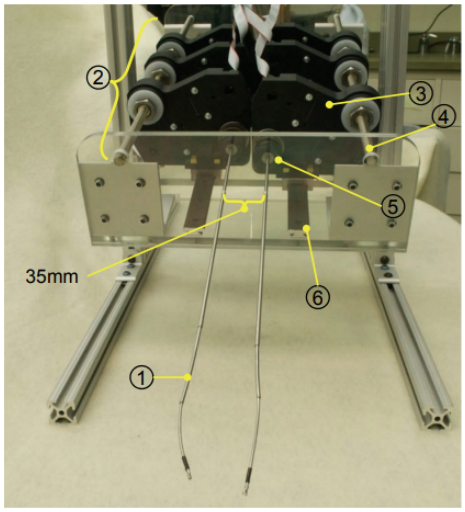

Figure 4: Cannula fastening solution using collets (pointer 5) [5]

2.6 Conclusion

Concluding the current chapter, concrete decisions will be made considering both literature solutions and the prototype's targets. The actuation chain that we chose is serial for its simplicity and cost effectiveness in comparison with parallel actuation. Although parallel actuation generally reduces the overall length of the tubes it multiplies the amount of rails and makes the design more bulky and costly. The issue of concentricity of the tubes is also worth keeping in mind when considering the parallel actuation design since multiple translating axes need to implemented. As far as general motor choice is concerned, we conclude that piezoelectric and pneumatic solutions, although extremely precise, tend to be complicated to control and quite expensive. For these reasons electromechanical actuation will be employed and in particular the design will be actuated by stepper motors. In the current application the generated noise during motion is not of big concern. In addition, high speeds will not be required neither really high loads making the choice of stepper motors ideal. The high holding torque of the stepper motors is also welcome so any interaction at the end effector does not translate to the positioning system. This also helps against the torsional energy stored in the tubes which acts as torque during operation which might require controlled breaking action in the case of BLDC motors. Furthermore the resolution of stepper motors can be increased using simple microstepping drivers further adding to the simplicity of the design for higher precision. Stepper motors for the actuation unit were used in [8] and amongst the goals of their design was cost-effectiveness which aligns with the aim of the current prototype. Both for translation and rotation, the prototype will make use of stepper motors (non-captive stepper motors for translation and hollow shaft motors for rotation) aiming for the most cost-effective and sim-

plicity. The prototype will make use of limit switches to ensure safety while operating. The limit switches will be used to perform a homing operation for the translation blocks as well at the start of every operation cycle. Finally, a solution for fastening the cannulas that has not appeared in the literature is the use of clamps. These components can be easily 3D designed and printed which constitutes a simple and cost effective solution. A clamp connected to the hollow shaft motor and another connected to the tube will be the target solution that we aim for. The two clamps will be screwed together in order for the tubes to be rigidly connected to the hollow motor shaft. This design choice will allow the prototype to have the option of hosting different tube diameters on demand simply by 3D printing new clamps which furthers its flexibility. Figure 5 illustrates an overview of the design choices made for the prototype. Green outline illustrates the choice for the current prototype and red outline is the rejected or not utilised approach. It is worth mentioning that not all choices for the same topic are mutually exclusive, e.g. for sensing multiple choices could be made.

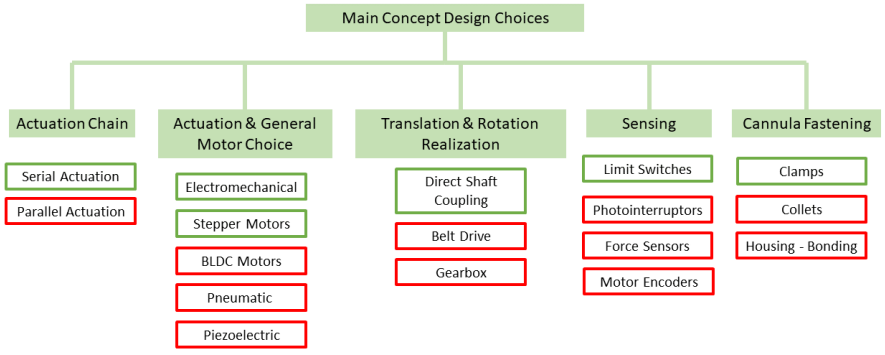

Figure 5: Design Choices Overview

3 Prototype Overview

The final concept of the robot will consist of translating stages riding on sliders which rest on a guide rail (Part number: HSR20A5+500LH, MISUMI Europa GmbH). The stages carry a pair of stepper motors each, one for translation of the stage and one for rotation of the cannula attached to the stage. The stepper motors will be driven by microstepping drivers which in turn will be controlled by an Arduino Mega 2560. The 3D model of the system can be seen in 6a and the realization of the prototype in 6b and 6b. One of the goals was to design

the prototype in a modular fashion. The proposed design scheme allows the use of up to four stages (i.e. four concentric tubes) without significant changes of hardware/software, simply by adding additional stage assemblies to the guide rail. The currently presented prototype shows two stages that ride on the same guide rail.

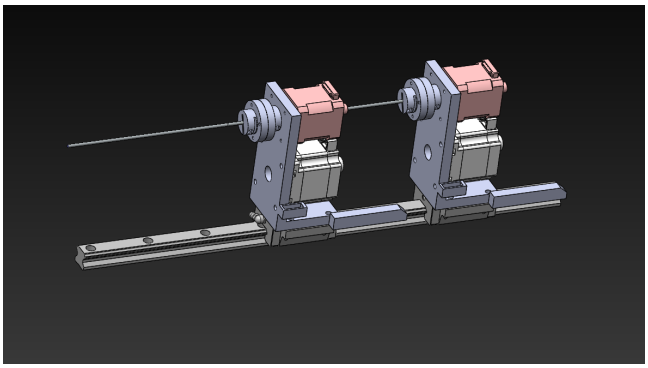

(a) 3D model of the prototype

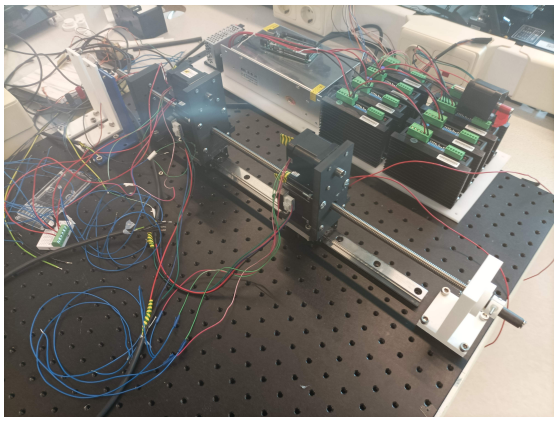

(b) Prototype realization

Figure 6: Prototype overview

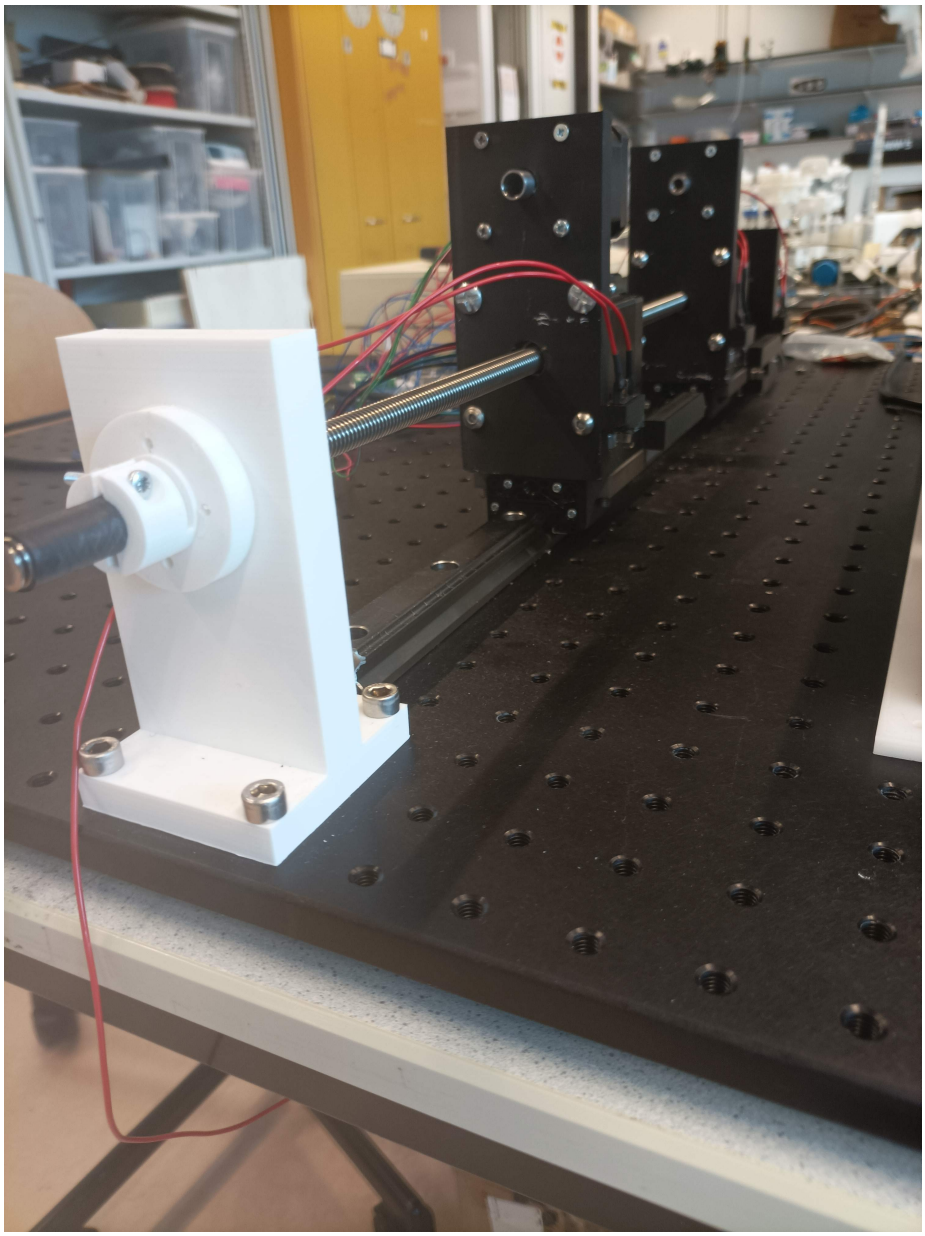

Figure 7: Prototype realization - Aspect

3.1 Stage Design

The stage (also referred as actuation block) is a central part of the design. It accommodates two motors, one for translation of the whole block and one for

rotation of the cannula attached to it. In figure 8 both the actual and 3D model of the stage can be seen as well as the stage, motor and limit switch assembly (firing pin and limit switch housing). The volume footprint of the assembled stage measures approximately 70 X 40 X 100 mm (L X W X H in mm). It is worth noting that the firing pin is not included in the footprint as it does not structurally affect the motion of the stages, the same applies for the switch housing. The switch housing is used to hold the limit switch in place while the firing pin flips the limit switch of the previous stage during homing or during abnormal operation to avoid collisions.

3.2 System Specifications

For the translation of each stage non-captive stepper motors (LA561S20-B-TSCA, Nanotec Electronic GmbH & Co. KG, Munich, Germany) were used that translate on a lead thread. The thread is clamped at both ends to avoid unwanted rotation and translation during the motor operation. For the rotation of the cannulas, each stage is equipped with a hollow shaft stepper motor (model 17HS2048, Dings' Motion, USA). The hollow shaft works perfectly for the proposed cascaded design approach. In order to make the design simpler and limit the amount of moving components the cannulas are fastened directly on the shafts of the motors using one-ended clamps that connect with each other and while their exposed sides connects to the motor shaft and the cannula respectively. The stages rest on sliders that translate on a linear guide rail that has total length of 500mm. Table 1 illustrates the central specifications of the prototype.

Table 1: Specification Table

	Quantity	**Units**
Number of Stages	2 - 4	
Thread Pitch	2	mm
Linear motor resolution (w/out microstepping)	0.01	mm/step
Rotational motor resolution (w/out microstepping)	1.8	degrees/step
Rail Length	500	mm
Active rail length	300	mm

Velocity & Force Specifications

The translational and rotational velocity that the prototype is able to deliver is affected by the motor specifications. In figure 9 the force/velocity of the non-captive linear motors can be seen. Depending on the expected force feedback, translational velocity can be set from 1 mm/s to 30 mm/s. For testing and validation purposes of the prototype the speed will remain at 1 mm/s.

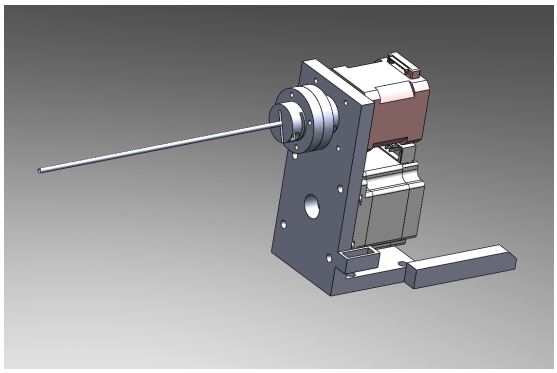

(a) 3D model of the stage assembly

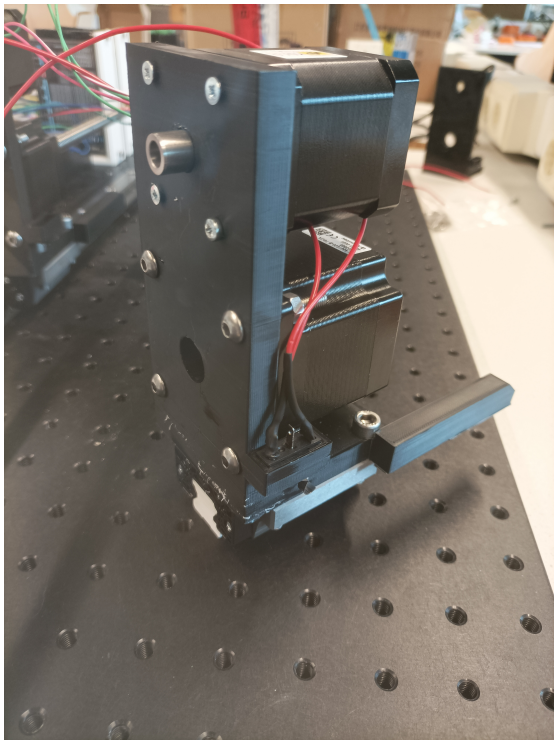

(b) Stage assembly realization

Figure 8: Stage Assembly

The torque-velocity curve of the hollow shaft motors (model 17HS2048) can be seen in figure 10. It is obvious that for speeds below 750 RPM the torque remains above 0.25 Nm. This value was qualitatively chosen in [5] as the lower bound for a design to be used in skull base surgery. The goal of the present design is bladder inspection so the end-effector, under normal circumstances,

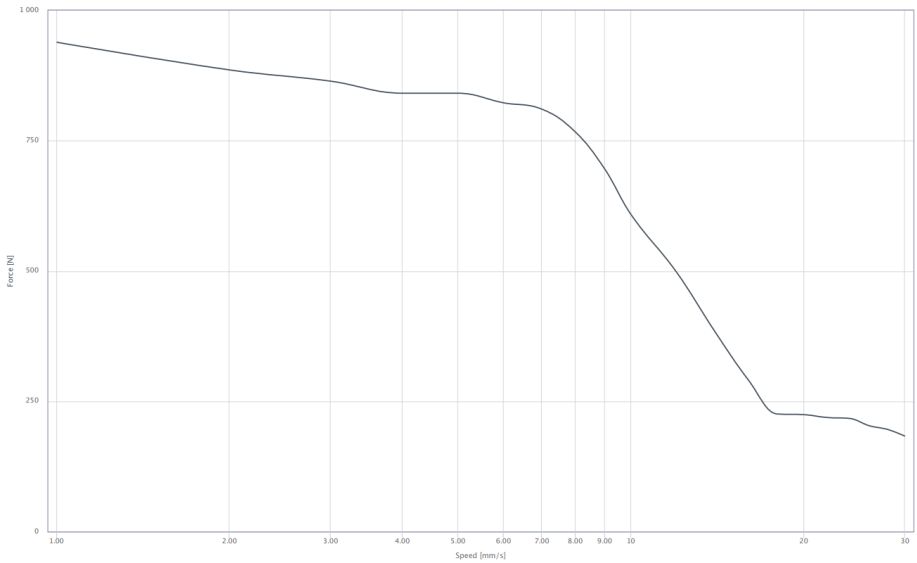

Figure 9: Linear Motor Force-Velocity Plot

should not interact heavily with the surrounding tissue. In this case we could consider even lower force/torque specifications as the design baseline.

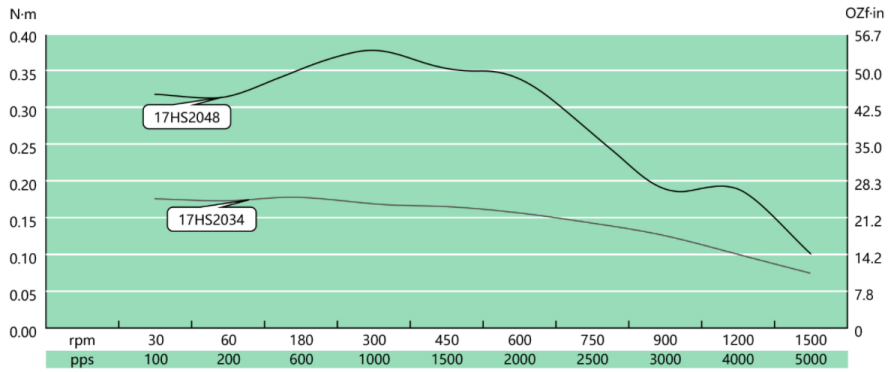

Figure 10: Rotational Motor Torque-Velocity Plot

Total Weight, Volume & Cost

In assessing the compactness of the design the total weight and volume of the design are crucial. The aim is to move towards a design that is as compact as possible and weighs as little as possible. The total weight is estimated to be

around 5 kg. The volume resembles a cuboid with approximate edge dimensions of 700 X 120 X 80 (Length X Height X Width) in millimetres. Table 2 shows an approximate cost total. This cost is obviously affected by the supplier of the components and this is the reason it is not concrete, yet this small overview allows for a good cost estimate. It is also worth mentioning that the 3D printed components, wires and other small electrical components are not included in the cost overview and in addition their contribution to the final cost is deemed insignificant. The total cost is extremely when considering that some alternatives in literature were in the range of tens of thousands of euros.

Component	**Price in euros**
Guide Rail w/ four sliders	530
4 X Non-captive Linear Stepper Motors	330
4 X Hollow Shaft Motors	220
Power Supply	50
Arduino Mega 2560	40
Total Amount	1170

Table 2: Approximate Realization Cost

Total Translation Constraints

The rotation of the cannulas is free of any constraint since their are structurally independent, however this is not the case for the translation of the stages. The present guide rail totals 500 mm in length however not all of it is actually utilized. When a slider is at the back end of rail the base of the attached cannula is approximately 60 mm in front of the rail's end and in essence this distance is not utilized at all during operation. When the stage stands in the back end the cannula is protruding (in relation to the rail's front end) so it adds approximately 20 mm of usable clearance. So the total amount of possible translation for one slider is 460mm. Since the prototype is supposed to operate with two to four stages on the same rail the total clearance for each stage needs to be calculated again. Each stage has a length of 70 mm so in the case of two stages in total the active clearance is recalculated to 460 mm - 70 mm = 390 mm and then divided by two under the assumption that both stages need to be able to move the same total distance, makes the clearance for each stage 195 mm. The same calculation leads to the results illustrated in table 3. The clearance provided by each configuration (i.e. two, three or four stages and subsequent tubes) plays a role in the design of the tubes and more specifically to their total straight and curved lengths as well as the position where the curve of each tubes begin. The design of the tubes play a crucial role in the reachable workspace of the robot and need to be considered carefully.

# of Stages	Individual stage clearance (mm)
1	460
2	195
3	106
4	62

Table 3: Clearance and stage quantity

Cannula Clamp Design

Figure 11 illustrates the 3D designed cannula clamps.The motor shaft clamps differ only in the hole diameter. The center holes of these clamps are designed with a diameter that changes one mm before the end to a smaller diameter. This is necessary to ensure both the motor's shaft and the the nitinol tube are always the same distance apart which is necessary for the translational accuracy of the device.

3.3 Control & Communication

In order to control the motors of the actuation unit an Arduino Mega 2560 prototyping board was used in conjunction with stepper drivers that offer different microstepping resolutions as well as circuit protection (e.g over/under-current, open-circuit detection) and appropriate heat sinking (model SL2690A 2 Phase Hybrid Stepper Drives Shenzhen Penhui Technology Co., Ltd). Dedicated software was developed for the control of the different stages as well as the communication of the robot with the user.

The immediate control of the motors present in the actuation unit occurs through the Arduino Mega 2560. The prototyping board is responsible for sending control signals to the stepper motors through the drivers. Setting up the motion specifications such as speed, microstepping resolution, etc. takes place in the Arduino environment (as far as software is concerned) but the microstepping resolution needs to match the one selected physically through switches of the drivers. The motors can be controlled by sending the appropriate commands through the Arduino's serial port either using the Arduino IDE serial port or using Matlab. A communication routine was developed to allow this both for use during development since it made the experiments much easier to automate and also because looking ahead the Arduino will need to communicate with a top-level controller which is going to be issuing commands to it, in order to reach a specific end-effector pose. The Matlab-Arduino communication was developed in such way that the Arduino can both automatically "read" values from a matrix format that correspond to move commands of the motors and also the user can issue move commands at will, depending on the mode of communication. Figure 12 shows the wiring schematic for one motor configuration. We control the positive ends of both the direction pins and the step(/pulse) pins of the

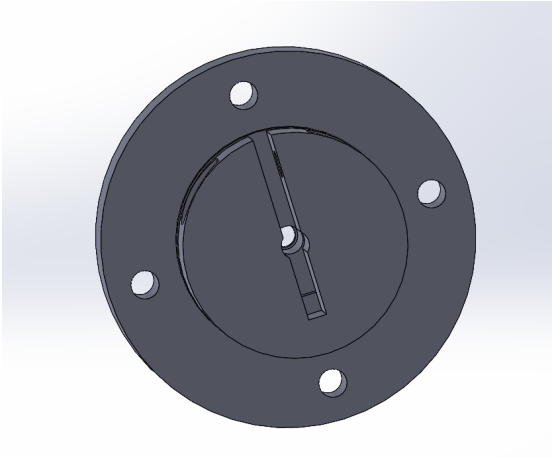

(a) 3D model of the tube clamp - aspect 1

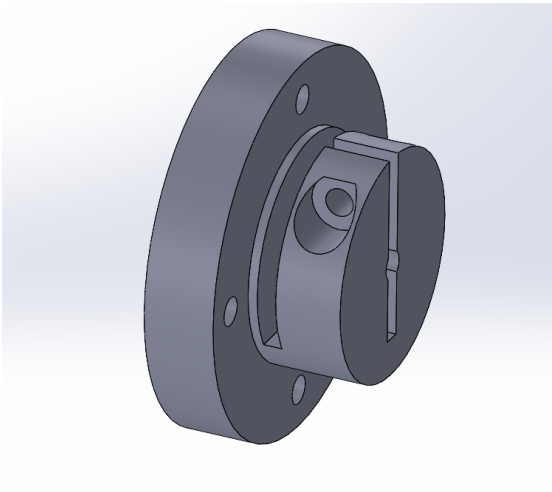

(b) 3D model of the tube clamp - aspect 2

Figure 11: Tube Clamp

driver while the negative pins are grounded. The enable pins of the driver are not utilised.

The Accel Stepper library is an already implemented library which allows the creation and control of stepper objects. This library aside from classic step and speed control also allows acceleration control and multi-stepper control, which is currently utilised by the setup. At the current stage of development the robot accepts move commands for all the motors present and executes the movement pseudoparallel, meaning that all motors begin and end their movement at the same time after an issued commands, they move at different speeds

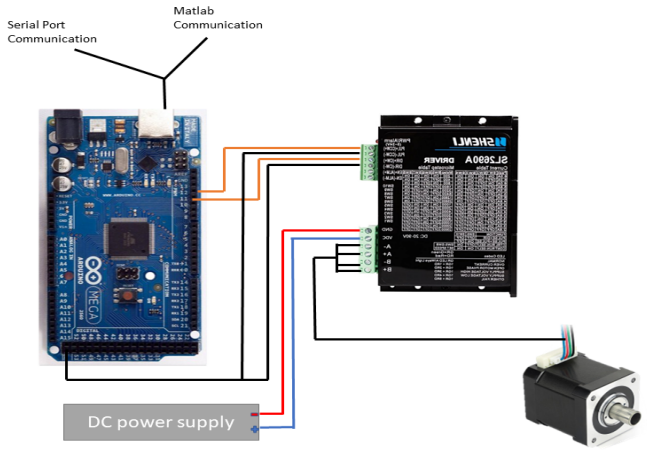

Figure 12: Wiring Diagram

depending on the travel distance however at any given moment only one stepper is stepping. The motion appears concurrent due to the swift switching that takes place when issuing step commands to the motors. Single motor control is also possible through this mode.

The communication with Matlab is established through a one-way channel at the moment, where Matlab sends a move command through the serial port to the Arduino which is always looking for issued commands. After the command is issued Arduino initiates movement and sends some diagnostic data back to Matlab however it does not control Matlab execution nor can halt it. Figure 13 shows a schematic representation of the communication sequence. It is important to note that while a movement is taking place the program execution in Arduino is blocked until the movement is successfully complete or a hardware interrupt is triggered due to a limit switch being pressed, which ultimately stops the movement of the motors

4 Experiments & Results

The goal of the following experiments is to validate the accuracy and precision of the prototype. First the noise level of the NDI system will be investigated. Then a single stage validation will take place, where using the NDI sensor, the translation and rotation of a rigid 3D printed tube attached to the stage will take place. Different motion intervals will be considered in repeatability tests. The results will be presented in scatter plots and tables illustrating the mean error and standard deviation for each movement both for translation and rotation along with possible drift derived from a least-squares approach. Finally

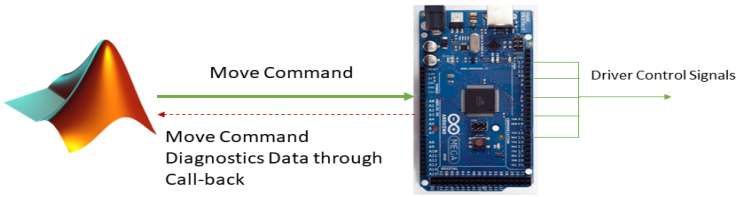

Figure 13: Control Schematic

a translational homing repeatability experiment will be carried out to test the accuracy of the homing and calibrate the interstage distance after homing.

The NDI system provides absolute 3D pose data for the sensor in its magnetic field. The six dimensional data include three translations and three rotations expressed in its fixed Cartesian coordinate system which is set by the manufacturer. In the analyses that follow, the data shown, are either expressed in the global coordinate frame or they have been transformed to the sensor's local coordinate frame using the first obtained datapoint as the start of the experiment or subsequent movement. The reason this transformation takes place is for the obtained datapoints to reflect movement in relation to the starting sensor position rather than the global coordinate frame. The Z-axis of the local system always points in the direction of translation while the two other axes' orientation are not known (a trivial fact for our experiments) since they depend on the orientation of the sensor along its axis of symmetry (Z-axis). The exact orientation could be inferred but it does not affect the results of the experiments that were carried out. The experiments were carried out using a microstepping resolution of 800 meaning that each step amounts for 0.0025 mm translation and 0.45 deg rotation depending on the evaluated module.

4.1 NDI system noise evaluation

For the first experiment, the noise of the NDI system will be evaluated. The sensor remained stationary (no translation or rotation occured) for twenty minutes while the system collected 3D pose data. These datapoints are expressed in the global coordinate frame of the system. The NDI system takes approximately fourty measurements every second. This amounts for an approximate amount

of 48.000 datapoints collected. After the data collection was completed, post processing took place and namely the datapoints were transformed to the local coordinate frame of the sensor, the mean of the data was removed and the standard deviation was calculated. The data was evaluated for possible significant trends. If a trend was observed it was removed by approximating it with a first order polynomial (i.e. the assumption of a linear drift was made). The results can be seen in figures 13, 15 and in tables 4, 5. Figures 13d, 15d show examples of the trends present in the noise data, that were ultimately removed.

Axis	**Standard Deviation (mm)**
X	0.0186
Y	0.0181
Z	0.0188

Table 4: Translation Noise signal standard deviations

Axis	**Standard Deviation (degrees)**
X	0.0246
Y	0.0742
Z	0.0137

Table 5: Rotation Noise Signal Standard Deviations

4.2 Translation & Rotation Repeatability Tests

The second round of experiments are focused in the repeatability the actuation system can provide under motion (translation and rotation). The values were obtained through repetitive movements of 1cm, 1mm and 0.1mm for translation and 9 deg, 4.5 deg and 0.9 deg for rotation. The intervals were chosen based on the estimated movement resolution that will be required during operation for a medical device of this type. Since safety and comfort of the patient are of major concern the sequential movement commands will be around the millimeter and degree level. The system was ordered to move between absolute positions for the corresponding intervals two hundred times. The results obtained from the tests were transformed to the local coordinate frame each time the system returned to the initial position in order to counteract any noise trend from influencing the integrity of the data. Should the actuation system exhibit any trends e.g. by missing steps or backlash this will become obvious by evolution of the mean of the measurements. A least-squares line will be fitted to the data and an evaluation will be made on how many steps the system could be missing/overshooting. We expect to see a standard deviation with magnitude similar to the identified noise in the previous chapter and a mean that is relatively close to our move command.

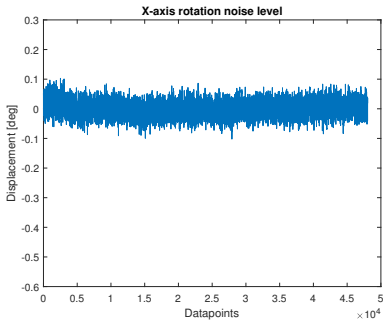

(a) X-axis rotation noise

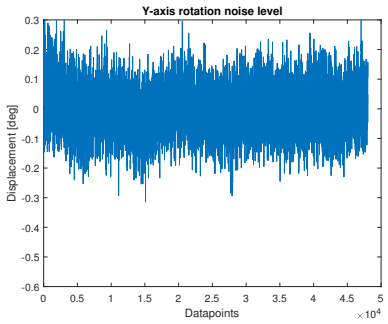

(b) Y-axis rotation noise

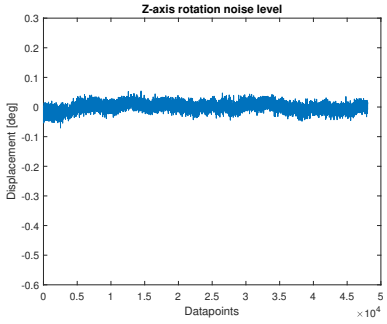

(c) Z-axis translation noise

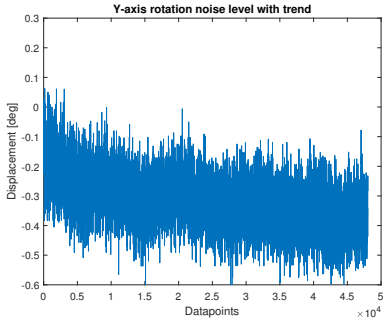

(d) Y-axis translation noise with trend

Figure 15: Rotation Noise Signal Measurements

Translation & Rotation Test Results

In figures 16 and 17, the scatter plots for the different translation/rotation intervals are illustrated. The datapoints were also used to fit a least-squares line for evaluating purposes. This line aims to show whether there is a significant trend in the collected data ultimately showing the need for calibration or the need for feedback control. In tables 6 and 7, the quantitative results are presented. The last column represent the amount of millimetres (/degrees) of drift that were theoretically accumulated during testing based on the collected data.

4.3 Homing Repeatability Tests

The third round of experiments involve translational repeatability of the homing operation for one stage. Homing was performed fifty times and the absolute position of the stage was evaluated each time. Figure 18 illustrates the collected datapoints and table 8 shows the corresponding derived metrics. The homing results will establish a baseline for the robot's translational accuracy.

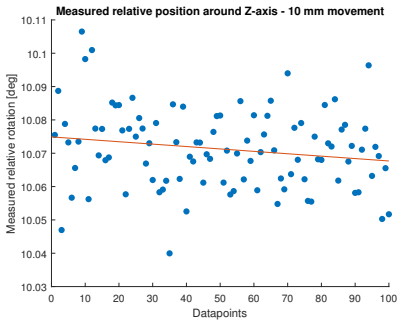

(a) 10 mm Linear Displacement

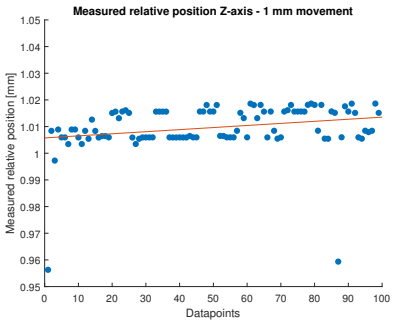

(b) 1 mm Linear Displacement

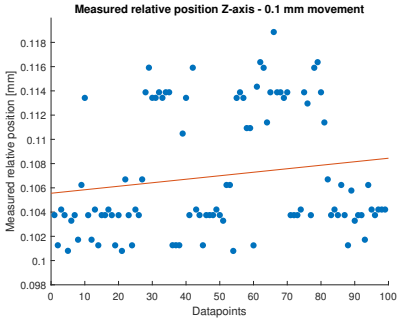

(c) 0.1 mm Linear Displacement

Figure 16: Linear Displacement Tests for Different Intervals

5 Discussion

This chapter starts with an analysis of the test results and continues with general results of the prototype paired with the initial goals set during the introduction as well as general points regarding the design of such actuation units derived from the approach followed for the realization of the presented prototype.

Test Results

The initial experiment of noise evaluation of the NDI system proved quite useful since there was moving average trend in some of the axes. Figures 13d and 15d are used as examples of this moving average phenomenon whose origin is not investigated further. The rest of the subfigures in figures 13 and 15 display detrended data for the motion on/around the different axes. The presence of a moving average noise signal dictated a specific approach when manipulating the data obtained from the translation and rotation precision tests that consequently took place. Namely each time the system returned to its starting position that position was considered the origin of the sensor's coordinate frame

Experiment Metrics			
Movement interval [mm]	mean [mm]	std [mm]	least-squares drift [mm / 100 rep]
10	10.0109	0.0104	-0.0085
1	1.0096	0.0091	0.0078
0.1	0.1070	0.0051	0.0029

Table 6: Mean, Standard Deviation and Drift - Translation

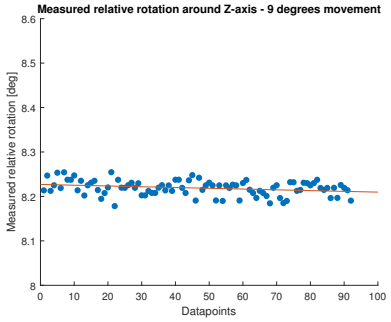

(a) 9 Degrees Angular Displacement

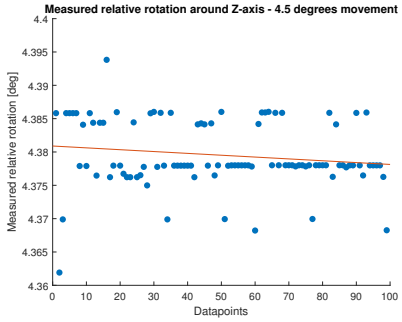

(b) 4.5 Degrees Angular Displacement

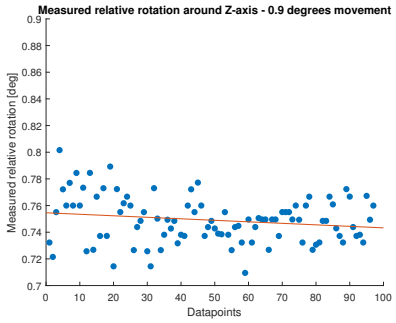

(c) 0.9 Degrees Angular Displacement

Figure 17: Angular Displacement Tests for Different Intervals

(local coordinate frame). The important metrics derived from the noise analysis is the standard deviation of the noise signal in the system which had an order of magnitude of 10e-2 mm and 10e-2 degrees. This allows for a more informed conclusion when it comes to the evaluation of the precision of the system which was the topic of the next cycle of experiments. In figures 16 and 17 the results of the precision tests are graphically presented however tables 6 and 7 provide a more quantitative view of the results. The conclusion from these results is that the actuation unit can be operated with relatively good precision arguably sub-

Experiment Metrics			
Movement interval [deg]	mean [deg]	std [deg]	least-squares drift [deg / 100 rep]
9	8.2189	0.0168	-0.0173
4.5	4.3795	0.0050	-0.0028
0.9	0.7490	0.0175	-0.0113

Table 7: Mean, Standard Deviation and Drift - Rotation

Homing sequence experiment metrics	**(mm)**
Mean	0.0046
Std	0.0157

Table 8: Homing Experiment Results

millimeter for translation and close to degree precision for rotation. The mean values of the different motion intervals are relatively close to the commanded ones and their deviation occurs in a lower order of magnitude than what the NDI system would allows us to confidently measure. This can be seen from the order of magnitude of the standard deviations in the result tables. The same applies for the drift whose values seem to be insignificant in relation to the order of magnitude of the introduced system noise. The need for a 6D measuring system with less noise should be considered to evaluate the actuation unit's precision capabilities with greater confidence. The homing repeatability results in figure 18 and table 8 also illustrate that the accuracy of the homing precision is submillimeter but more robust testing is required to in order for the measured results to be significant. It is worth noting however that from literature the kinematic modelling of the tubes that is used for control introduces inaccuracies around two orders of magnitude larger than the ones presented for the prototyped actuation unit and in essence it should allow for accurate estimation of different kinematic models' precision.

Accuracy & Precision

The precision of the actuation unit has been verified to be submillimiter for translation and around a single degree for rotation through the series of tests presented in the previous chapter. However more tests need to be carried out with instruments of higher accuracy, to robustly verify submillimeter (subdegree) precision. The same thing does not apply for its overall accuracy. For accuracy (knowledge of absolute positioning) the system needs to know the exact pose of each one of its actuation blocks (referring to translation of the stage and the rotation to the cannula). The translating block offers a degree of accuracy through the use of limit switches to perform a homing operation. Once

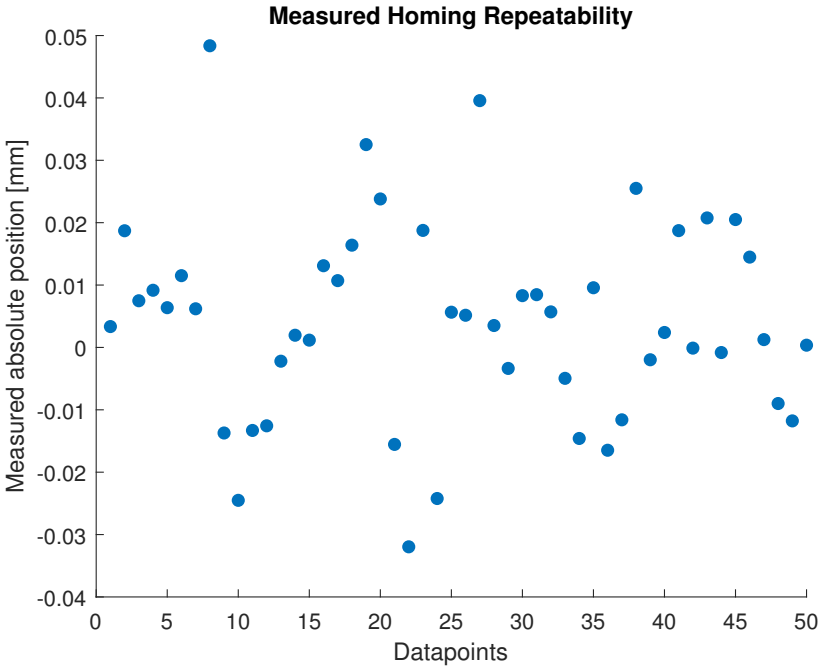

Figure 18: Homing Repeatability Experiment Datapoints

calibrated the system can achieve good translational accuracy however the applied method is not the most robust. Both the use of different limit switches could further increase the accuracy of the translation and also a more robust calibration method can be applied to ensure the accuracy is in an acceptable range for the application. When it comes to rotational accuracy the system does not provide any option. From literature, photointerruptors have been used for rotational homing that theoretically provides the necessary accuracy however it does not take into account the accuracy of the fastening at the assembly stage of the design. If the accuracy is compromised on that level then photointerruptors only provide repeatable results for the rotor's angle and not necessarily overall accurate one when considering the tubes' orientation. Again calibration through different means (e.g. through magnetic/laser sensors or stereo vision camera array) could solve this problem but that implies that calibration needs to take place before each use something that requires extra equipment and software which generally is against the aims of this prototype.

Cost Effectiveness

The resulting prototype seems to have achieved our initial goal of relative cost effectiveness (when compared to other prototypes). The general cost of the de-

sign ranged between 2000 and 2500 euros which is a considerable optimization for these kinds of robots. That being said, the cost can be decreased even further through the use of custom-made and (hopefully in the future) more informed solutions. For example the design of simpler stepper drivers could reduce the cost quite a lot. When looking at the capabilities of the current drivers, it is clearly visible that most of their operating capabilities are not utilized. The integrated circuit protection and a few of the microstepping resolutions are the only necessary requirement. While testing it was also observed that the temperature never rose significantly in the drivers, so their heat sinking capabilities where not fully utilised or needed. Smaller motors could theoretically be used for the actuation blocks however the specifications for these kinds of prototypes are rather vague and the handful of authors that consider force and torque specifications result in using qualitative approach into determining those values, which is obviously a start but definitely not the optimal approach. There is a lack of research when it comes to such specifications so it is not necessarily clear on how to approach such a subject. The force/torque specifications also change depending on the procedure the robot will be involved in, e.g. if the robot needs to interact with its environment for surgery purposes it requires more force/torque as opposed to a robot that only performs inspection through cameras, which is also the goal of the current prototype. Most of the structural components are 3D printed which also helps the design maintain a relatively low cost footprint.

Design Flexibility, Compactness & Ease of Use

The resulting design is quite flexible in the sense that it can host up to four cannulas (resulting in eight degrees of freedom as far as the actuation unit is concerned) with relative ease during reconfiguration and general assembly. Its main structural components can be 3D printed using any preferred material. Furthermore it has a relatively small volumetric footprint and low weight meaning that it can be fastened on tabletop or even a robotic manipulator, as often happens with such devices during medical procedures. The actuation unit can be controlled in a variety of modes through the Arduino serial port. Although this provides a relatively easy way of controlling the prototype during design and validation stage it does not provide a user-friendly environment. In addition, considering that the design needs to operate with a top level controller, that incorporates solutions for the flexible body kinematics, it becomes quite obvious that a more flexible communication procedure is required.

General Points & Considerations

An obvious shortcoming of the design is the abundance of cables present. Under wrong handling they could be damaged or cause a failure of the design if not managed correctly. This issue is mentioned by other authors who constructed such prototypes. Proper cable management will result in a safer design easier to further optimize, upgrade and troubleshoot. A robust solution is required

for this issue. Another important aspect that was highlighted during the design procedure was the need for initial workspace design. The workspace of the end-effector plays an important role in the specifications of such prototypes, as it introduces additional constraints for the translation of the individual tubes and ultimately the clearance each stage should have in order the end-effector to be able to move in the designed workspace. This workspace is of course procedure specific (and also patient specific in some cases) and an initial estimation can introduced necessary constraints for the actuation system. Finally the forces/torques the end-effector and the body of the tubes will experience during operation need to be estimated. From literature, authors have tried to estimate such forces/torques qualitatively which is bound not to be precise, aside from the fact that this estimation is again procedure specific. If the end-effector is supposed to interact with the environment through miniature tools then higher forces are to be expected than the case where the robot is used for inspection purposes as is the case for bladder cancer detection. This estimation could play a role in realizing such prototypes with motors of different capabilities ultimately effecting the precision, size, weight and cost of the prototype. Microstepping is an excellent way to increase resolution however it does not come without drawbacks. Although the movement is made smoother when microstepping, effectively lowering vibration magnitude and general wear (especially on the linear component) it is not as resilient to outside forces as a full step, meaning that when the motor is in an intermediate step it does not produce the expected holding torque. In addition the maximum speed the microcontroller can deliver goes lower as the microstepping resolution increases. This happens because the motors' rotation is controlled by a PWM signal whose frequency dictates the speed of stepping. The frequency increases when the necessary steps for a full revolution increase due to microstepping and the microcontroller always has a upper limit on the maximum PWM frequency it can deliver affected mostly by its internal clock.

6 Conclusion

The realized prototype shows great promise as arguably the most cost-effective and simple (at least compared to literature), without compromising precision and possibly in the future accuracy. Namely, the use of low cost stepper motors for actuation appears to be an interesting choice when considering cost, complexity and precision. The simple cannula fastening solution employed aligns perfectly with the goals of this project and furthers its simplicity. In addition the prototypes design allows for great flexibility in the amount of tubes that can be used and their corresponding diameter. The first iteration of such actuation unit provides grounds for further development towards a unit that accomplishes the design goals of the present prototype to greater extend.

References

[1] Hessa Alfalahi, Federico Renda, and Cesare Stefanini. Concentric tube robots for minimally invasive surgery: Current applications and future opportunities. *IEEE Transactions on x‘ Robotics and Bionics*, 2:410–424, 2020.

[2] Stephanie Amack, Margaret F. Rox, Jason E. Mitchell, Tayfun Efe Ertop, Maxwell Emerson, Alan Kuntz, Fabien Maldonado, Jason A. Akulian, Joshua B. Gafford, Ron Alterovitz, and Robert J. Webster. Design and control of a compact modular robot for transbronchial lung biopsy. In *Medical Imaging*, 2019.

[3] Mohamed Nassim Boushaki. Design optimization and control for concentric tube robot in assisted single-access laparoscopic surgery. (optimisation de la conception et commande de robot à tubes concentriques pour la chirurgie laparoscopique par accès unique). 2016.

[4] Jessica Burgner-Kahrs, Daniel Caleb Rucker, and Howie Choset. Continuum robots for medical applications: A survey. *IEEE Transactions on Robotics*, 31:1261–1280, 2015.

[5] Jessica Burgner-Kahrs, Philip J. Swaney, Daniel Caleb Rucker, Hunter B. Gilbert, Scott T. Nill, Paul T. Russell, Kyle D. Weaver, and Robert J. Webster. A bimanual teleoperated system for endonasal skull base surgery. *2011 IEEE/RSJ International Conference on Intelligent Robots and Systems*, pages 2517–2523, 2011.

[6] Diana C. Cardona. A mri compatible concentric tube continuum robot with pneumatic actuation. 2012.

[7] David B. Comber and Eric J. Barth. Precision position tracking of mr-compatible pneumatic piston-cylinder using sliding mode control. 2011.

[8] Shunmugasundar Esakkiappan, Bijan Shirinzadeh, and Weichen Wei. Development of a cost-effective actuation unit for three dof concentric tube robot in minimally invasive surgery. *2019 IEEE/ASME International Conference on Advanced Intelligent Mechatronics (AIM)*, pages 1013–1018, 2019.

[9] Néstor Falcón, Sorush Ranjbar, E. Cisneros, Bao Huy Vu, Austin Schoppe, P. S. Pedro Sánchez, Yu-Fang Jin, JingYong Ye, Yusheng Feng, Dharam Kaushik, and R. Lyle Hood. Innovative computer vision approach to 3d bladder model reconstruction from flexible cystoscopy. In *BiOS*, 2019.

[10] Muhammad Umar Farooq, Binxiang Xu, and Seong Young Ko. A concentric tube-based 4-dof puncturing needle with a novel miniaturized actuation system for vitrectomy. *BioMedical Engineering OnLine*, 18, 2019.

[11] Hunter B. Gilbert, Daniel Caleb Rucker, and Robert J. Webster. Concentric tube robots: The state of the art and future directions. In *ISRR*, 2013.

[12] Richard J. Hendrick, S. Duke Herrell, and Robert J. Webster. A multi-arm hand-held robotic system for transurethral laser prostate surgery. *2014 IEEE International Conference on Robotics and Automation (ICRA)*, pages 2850–2855, 2014.

[13] Maximilian Christian Kriegmair, Tobias Bergen, Manuel Ritter, Philipp C Mandel, Maurice Stephan Michel, T. Wittenberg, and Christian Bolenz. Digital mapping of the urinary bladder: Potential for standardized cystoscopy reports. *Urology*, 104:235–241, 2017.

[14] Anke Richters, Katja K.H. Aben, and Lambertus A. Kiemeney. The global burden of urinary bladder cancer: an update. *World Journal of Urology*, 38:1895 – 1904, 2019.

[15] Hao Su, Diana C. Cardona, Weijian Shang, Alexander Camilo, Gregory A. Cole, Daniel Caleb Rucker, Robert J. Webster, and Gregory Scott Fischer. A mri-guided concentric tube continuum robot with piezoelectric actuation: A feasibility study. *2012 IEEE International Conference on Robotics and Automation*, pages 1939–1945, 2012.

[16] Hao Su, Gang Li, Daniel Caleb Rucker, Robert James Webster III, and Gregory Scott Fischer. A concentric tube continuum robot with piezoelectric actuation for mri-guided closed-loop targeting. *Annals of Biomedical Engineering*, 44:2863–2873, 2016.

[17] Philip J. Swaney, Jordan M. Croom, Jessica Burgner, Hunter B. Gilbert, Daniel Caleb Rucker, Robert J. Webster, Kyle D. Weaver, and Paul T. Russell. Design of a quadramanual robot for single-nostril skull base surgery. 2012.

[18] Philip J. Swaney, Arthur W. Mahoney, Andria A. Remirez, Erik P. Lamers, Bryan I. Hartley, Richard H. Feins, Ron Alterovitz, and Robert J. Webster. Tendons, concentric tubes, and a bevel tip: Three steerable robots in one transoral lung access system. *2015 IEEE International Conference on Robotics and Automation (ICRA)*, pages 5378–5383, 2015.

[19] Oktay Ucer, Gökhan Temeltaş, Bilal H Gumus, and Talha Muezzinoğlu. Comparison of pain, quality of life, lower urinary tract symptoms and sexual function between flexible and rigid cystoscopy in follow-up male patients with non muscle invasive bladder cancer: A randomized controlled cross section single blind study. *International Journal of Clinical Practice*, 75, 2020.

[20] Ran Xu, Ali Asadian, Seyed Farokh Atashzar, and Rajnikant V. Patel. Real-time trajectory tracking for externally loaded concentric-tube robots. *2014 IEEE International Conference on Robotics and Automation (ICRA)*, pages 4374–4379, 2014.

[21] Ran Xu, Ali Asadian, Anish S. Naidu, and Rajnikant V. Patel. Position control of concentric-tube continuum robots using a modified jacobian-based approach. *2013 IEEE International Conference on Robotics and Automation*, pages 5813–5818, 2013.

[22] Yong Zhong, Luohua Hu, and Yinsheng Xu. Recent advances in design and actuation of continuum robots for medical applications. *Actuators*, 2020.